JOURNAL OF GEOPHYSICAL RESEARCH, VOL. 101, NO. B11, PAGES 25,423–25,436, NOVEMBER 10, 1996

Postrifting anelastic deformation around the spreading plate boundary, north Iceland 2. Implications of the model derived from the 1987–1992 deformation field

M. A. Hofton
Institute of Geophysics and Planetary Physics, Scripps Institution of Oceanography
La Jolla, California

G. R. Foulger
Department of Geological Sciences, University of Durham, Durham, England

Abstract.
A decade-long rifting episode that began in the Krafla volcanic system, north Iceland, in 1975 caused substantial, regional, postevent anelastic deformation. This was modeled as viscous relaxation in an elastic/viscoelastic structure by *Hofton and Foulger* [this issue]. The results from modeling the deformation detected in north Iceland have far-reaching implications both for local and regional processes and for the fundamental behavior of deformation around spreading plate boundaries in general. Tilt in the vicinity of the Krafla volcano fits the model well after 1988/1989 which suggests that the volcano magma chamber stopped inflating/deflating in 1988. A viscosity of 0.8 x 10^{18} Pa s was required to match the local tilt data, less than that predicted for north Iceland as a whole. Vertical motion measured using the Global Positioning System (GPS) 1987–1992 around the ice cap Vatnajökull is inconsistent with isostatic uplift. Using the elastic-viscoelastic model to predict motion in other regions of Iceland suggests that the deformation effects of the Krafla episode are significant in many parts of Iceland and should be taken into account when modeling deformation there. Though not a realistic plate boundary model, interesting complexities of the elastic-viscoelastic model are highlighted by deformation modeling of an infinitely long dike. This predicts that the amount of horizontal displacement close to the dike may exceed the amount of initial dike opening early in the spreading cycle. A more realistic approximation to the plate boundary in north Iceland, involving five overlapping segments that experience dike emplacements at discrete intervals, suggests that the width of the zone within which transient, time-dependent deformation occurs may be several hundred kilometers wide, considerably wider than the neovolcanic zone. A kinematic approach to describing plate motions is not appropriate close to spreading plate boundaries and elsewhere where the viscosity of the Earth is low.

Introduction

The Northern Volcanic Zone (NVZ) of Iceland is the locus of the present-day spreading plate boundary in north Iceland. It comprises five en échelon volcanic systems, each containing a central volcano within a fissure swarm (Figure 1). Rifting is episodic in Iceland. In the NVZ it occurs about every 100–150 years, and only one spreading segment is thought to be active at a time [*Björnsson*, 1985]. During a rifting episode, several meters of extension may occur in the fissure swarm over a period of a few years [*Björnsson et al.*, 1977; *Sigurdsson and Sparks*, 1978]. Such a rifting episode began in the Krafla volcanic system in 1975 and lasted about a decade [*Björnsson et al.*, 1977]. Major dike injections in the Krafla fissure swarm caused as much as 9 m of extension at the surface, accompanied by a similar amount of compression of the plates on either side [e.g., *Björnsson*, 1985; *Gudmundsson*, 1995]. Extensive Global Positioning System (GPS) measurements made

Paper number 96JB02465.
0148-0227/96/96JB-02465$09.00

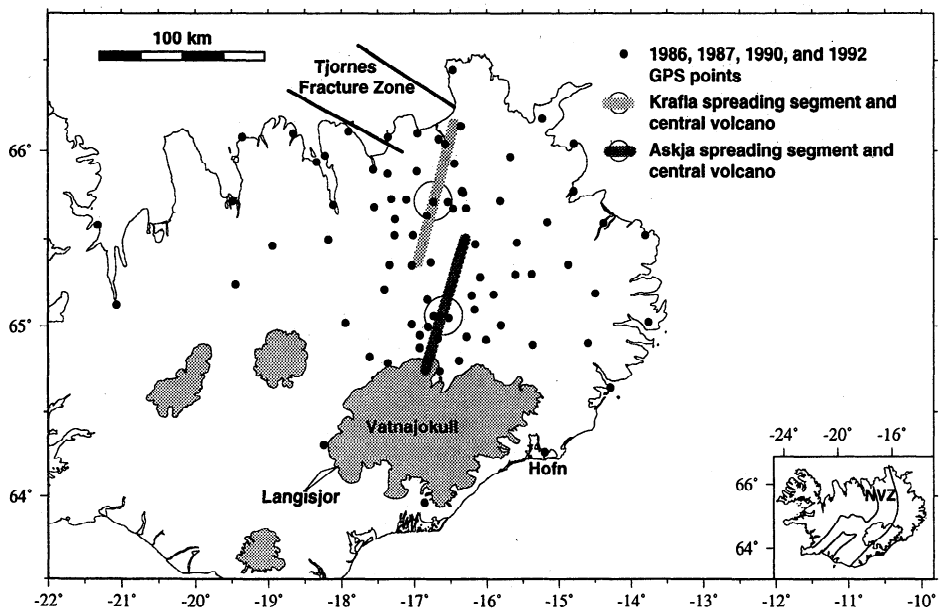

Figure 1. Map of Iceland showing the GPS points, two of the five en échelon volcanic systems of the Northern Volcanic Zone (NVZ), the Krafla and Askja volcanic systems, and features and place names referred to in the text. Inset shows the neovolcanic zone in Iceland.

after the episode in 1987, 1990, and 1992 detected substantial, regional, anelastic expansion [*Foulger et al.*, 1992; *Heki et al.*, 1993; *Jahn et al.*, 1994; *Hofton and Foulger*, this issue] at rates up to several times the time-averaged plate spreading rate of 1.8 cm/year [*DeMets et al.*, 1994].

The deformation field was interpreted as viscous relaxation of stress loaded on the region by the recent dike emplacements [*Foulger et al.*, 1992; *Heki et al.*, 1993]. *Hofton and Foulger* [this issue] modeled this postrifting stress redistribution using a structure involving an elastic layer overlying a viscoelastic half-space in which gravitational effects were included. A thickness of ~10 km for the elastic plate, a viscosity of 1.1 x 10^{18} Pa s, and an effective Maxwell relaxation time of 1.7 years for the north Iceland region were calculated, along with the dimensions of the dike intruded during the Krafla rifting episode.

In this paper we explore the implications of the elastic-viscoelastic model for both local and regional deformation in Iceland and for plate boundary processes in general. Models of tectonics at spreading plate boundaries have been hitherto heavily influenced by kinematic models that envisage continuous motion within a plate boundary region and the concept of events, e.g., earthquakes and dike intrusions, occurring in isolation. Ideas on the interdependence of plate boundary segments, triggering of events, and cyclic processes have been mentioned but rarely modeled quantitatively. The postrifting deformation observed in north Iceland enabled us to model part of the spreading cycle in detail and suggests important implications for both local deformation in north Iceland and plate kinematics in general. The predictions of this basic model can be tested where other observational data exist and, in future, using rapidly emerging new technologies, e.g., laser altimetry, synthethic aperture radar, and seafloor geodesy.

Implications for Local Processes in Iceland

Apparent Postrifting Inflation and Deflation of the Krafla Magma Chamber

Since 1986 an array of ground tiltmeters has been operated continuously in the Krafla area in order to monitor continued activity in the volcano. Data from these meters, which are all within 15 km of the Krafla caldera, indicate uplift and and subsidence that is variable both temporally and spatially [*Tryggvason*, 1994]. From early 1985, when the Krafla rifting episode essentially ended, to the end of October 1986, vertical ground movements at stations within 5 km of the Krafla caldera were negligible. From the end of October 1986 to March/April 1987, uplift occurred with the rate slowing until early 1989 when the sense of motion reversed and subsidence began. Subsidence continued until 1992. Stations 5–9 km from the caldera underwent uplift from 1985 to 1989 followed by no motion or very slight subsidence from 1989 to 1992. Stations more than 9 km from the caldera uplifted from 1985 to 1989 followed by no detectable motion from 1989 to 1992 [*Tryggvason*, 1994]. These observations were interpreted as indicating inflation of the Krafla magma chamber from 1985 to 1989, deflation of this same chamber from 1989 to 1992 accompanied by inflation of some deeper source,

and subsidence in the fissure swarm from 1985 to 1992 [*Tryggvason*, 1994].

Much of the ground tilt in the vicinity of the Krafla magma chamber following the end of the dike injection episode can be explained by viscous relaxation following the Krafla rifting episode. In order to fit the local tilt data, it was necessary to model the Krafla episode in more detail than was required to fit the regional GPS-determined deformation field [*Hofton and Foulger*, this issue]. Six discrete dikes, injected over a 5-year period were modeled, corresponding to the December 1975, October 1976, September 1977, January 1978, July 1978 and March 1980 events [e.g., *Tryggvason*, 1984]. The injection history was in reality more complicated than this [see, e.g., *Gudmundsson*, 1995], but the simplification used here is adequate for modeling purposes. The modeled dikes had thicknesses of 2.5 m, 1.2 m, 1.5 m, 1.2 m, 2.4 m, and 2.3 m and lengths of 44 km, 23 km, 38 km, 34 km, 35 km, and 34 km, respectively (dimensions inferred from the data of *Tryggvason* [1984]). The modeling method used was the same as used by *Hofton and Foulger* [this issue] to model the regional deformation field. The vertical motion was predicted for six, year-long intervals from 1986 to 1992 (Figure 2). A viscosity of 0.8 x 10^{18} Pa s was required to match the observed tilt data (Figure 3). This value is somewhat lower than the viscosity of 1.1 x 10^{18} Pa s used for the regional model [*Hofton and Foulger*, this issue]. Nevertheless, it is to be expected that the viscosity locally beneath the plate boundary, where hot material is thought to upwell, is somewhat lower than the regional average.

The results show that viscous relaxation following the Krafla rifting episode can account well for the observed

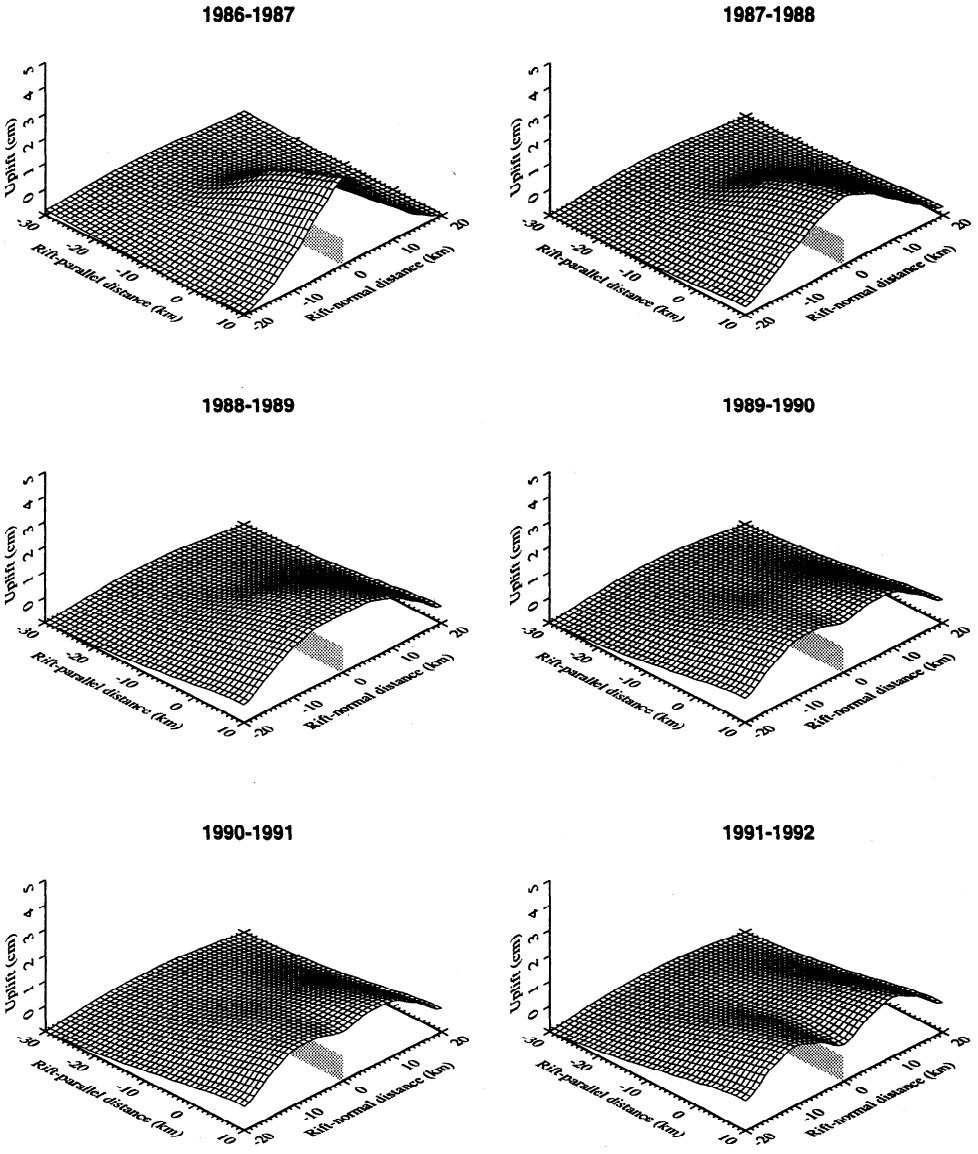

Figure 2. Predicted vertical motion during six, year-long intervals from 1986 to 1992 within a 40 km^2 area around the southern end of the dike intruded into the Krafla segment. The Krafla central volcano is situated at $x = y = 0$. The position of the dike is shown lightly shaded.

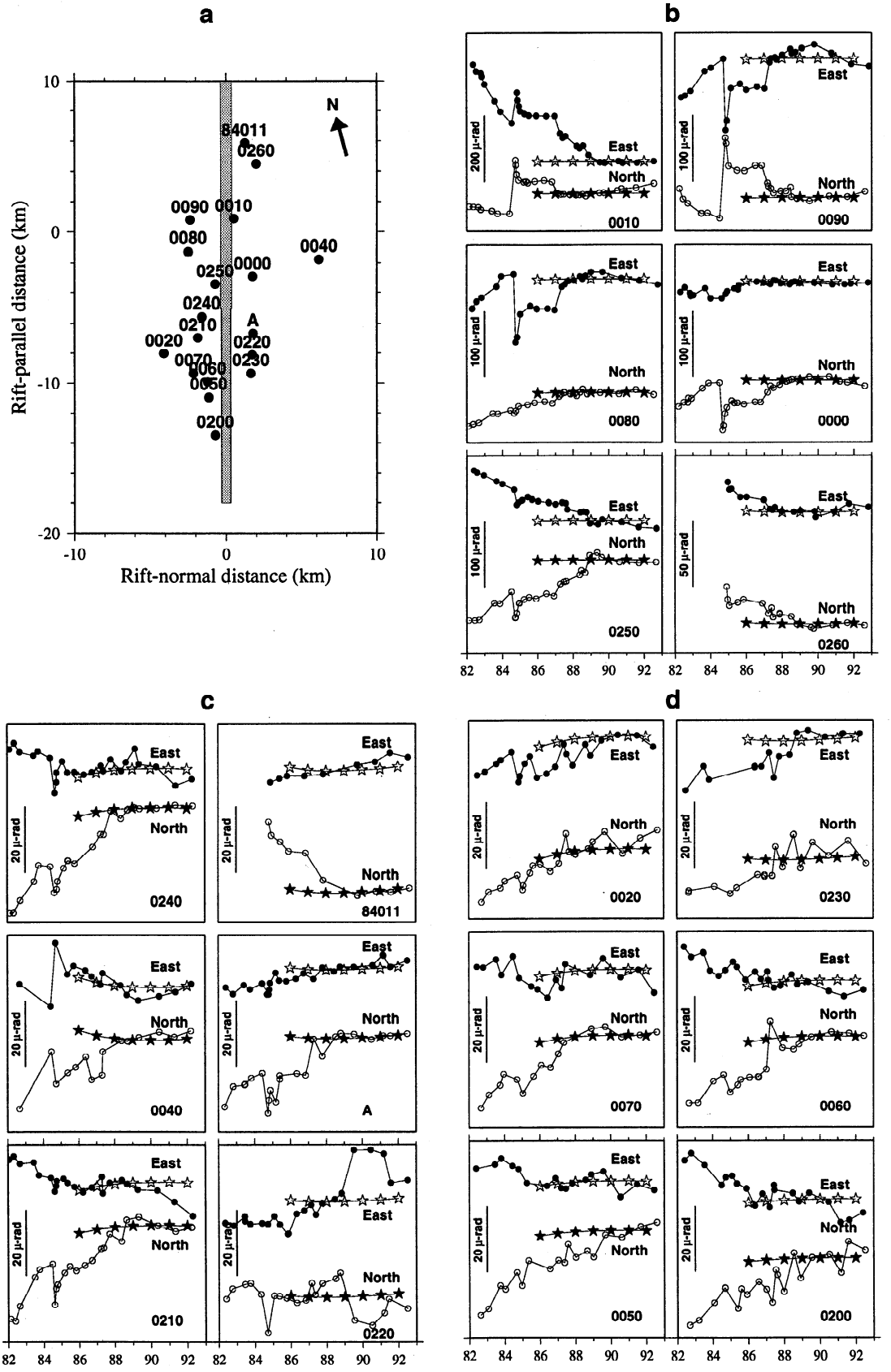

Figure 3. (a) Map of the Krafla area showing optical leveling tilt stations. The center of the Krafla central volcano is located at $x = y = 0$. Observed ground tilt from 1982 to 1992 and simulated tilt from Figure 2 are shown at optical leveling stations at distances of (b) less than 5 km, (c) 5–9 km, and (d) >9 km from the center of the volcano. The scale bars center left give the (variable) tilt scales. Increasing uplift is to the east (top curves) and north (bottom curves). The solid circles and open stars show the observed and simulated east tilt, and the open circles and solid stars show the observed and simulated north tilt. The observed tilt data and station locations are taken from *Tryggvason* [1994].

tilt data after late 1988/early 1989, and indeed, the predicted motions resemble strikingly those expected for an active (i.e., inflating and deflating) magma chamber. The model cannot account for the tilts prior to this time which must be due to some other process, e.g., inflation of the Krafla magma chamber [*Tryggvason*, 1994]. These results suggest that the Krafla magma chamber may have ceased its recent phase of activity in late 1988/early 1989.

Isostatic Uplift Around the Ice Cap Vatnajökull

Isostatic uplift is predicted to be occurring currently in southeast Iceland [*Sigmundsson and Einarsson*, 1992] following deglaciation since about 1930 when the ice cap Vatnajökull (Figure 1) began retreating in the wake of the Little Ice Age (~1450–1850) [*Grove*, 1988]. The area and volume of Vatnajökull are estimated to have decreased by 300 km^2 and 180 km^3, respectively, since 1930, inferred from estimates of length changes of outlet glaciers and Landsat images [*Sigmundsson and Einarsson*, 1992]. Modeling the Earth as a Newtonian viscous fluid half-space overlain by an elastic layer and assuming a spherical ice cap predicts 11.4 cm/year of thinning within the innermost 35 km of the ice cap, 23 cm/year between 35 and 47.5 km, and 57 cm/year from 47.5 to 52.5 km. This volume decrease is predicted to result in surface uplift immediately around Vatnajökull at a rate of 5–10 mm/year at the present time and tilt away from the ice cap if the viscosity of the asthenosphere beneath Iceland is in the range 1 x 10^{18}–5 x 10^{19} Pa s [*Sigmundsson and Einarsson*, 1992].

Figure 4a shows the vertical motions detected using GPS for the period 1987–1992, after removing the effects of the recent Krafla rifting episode and other tectonic events, described by *Hofton and Foulger* [this issue]. For comparison, Figure 4b shows the vertical motions at the GPS points predicted using the glacio-isostatic rebound model of *Sigmundsson and Einarsson* [1992]. Using a viscosity of 1 x 10^{19} Pa s, uplifts of up to 16 cm are predicted for the points closest to the northern and southern edges of the ice cap (Figure 4b). Predicted motion decreases with distance to reach zero at about 50 km from the perimeter of Vatnajökull. The majority of points in the network are thus unaffected by isostatic uplift according to this model. Viscosities of 1 x 10^{18} Pa s and 5 x 10^{19} Pa s would predict uplift of up to 23 and 8 cm, respectively, at the points of the GPS network and similar patterns of deformation to that shown in Figure 4b.

A comparison of Figures 4a and 4b clearly shows that the vertical motions observed for 1987–1992 using GPS bear little resemblance to those predicted by the isostatic uplift model. A circular pattern of uplift about Vatnajökull is predicted, whereas the dominant observed vertical deformation pattern is regional tilt up to the NNE. Only the motion at point Höfn (Figure 1) shows substantial uplift relative to, say, intraplate points distal to the west and east. Observational evidence cited in support of glacio-isostatic uplift around Vatnajökull comes from two sources. First, relative strandline elevations around Lake Langisjör (Figure 1), a glacial lake at the southwestern edge of Vatnajökull, indicate recent tilt upward toward the ice cap [*Sigmundsson and Einarsson*, 1992]. Second, recent shallowing of the harbor at Höfn, on the southeastern edge of Vatnajökull, was suggested to indicate uplift [*Einarsson et al.*, 1996]. The GPS results confirm these two observations. Uplift of Höfn is observed to have proceded at a rate of about 1.5 cm/year for 1987–1992, and the regional deformation pattern is consistent with uplift to the northeast for points southwest of Vatnajökull. However, the regional deformation pattern provides no evidence for systematic isostatic uplift centered on Vatnajökull.

Secular Deformation in Iceland

Traditional interpretations of motion around plate boundaries often involve identifying a zone within which transient, time-dependent motion occurs and outside of which motion is assumed to be continuous. Consider the deformation around the Askja volcanic system (Figure 1). An analysis of a subset of 15 of the GPS points occupied during 1987–1990 in the Askja region was used by *Camitz et al.* [1995] to infer the existence of a 30–45 km wide zone in the Askja volcanic system, within which the transient deformation signals of episodic motion are detected and beyond which points move at the full spreading rate. However, all of the displacement in the region can also be explained as viscoelastic stress redistribution following the recent Krafla rifting episode at better than the 2σ level (Figure 5).

Deformation Elsewhere in Iceland

The best fit viscoelastic stress redistribution model for the 1987–1992 deformation field in north Iceland [*Hofton and Foulger*, this issue] was used to predict motion from the recent Krafla rifting episode in the Tjörnes Fracture Zone (TFZ), the Askja area, the Eastern Volcanic Zone (EVZ), the Western Volcanic Zone (WVZ), the South Iceland Seismic Zone (SISZ), and the Reykjanes Peninsula for 1987–1992 (Figure 6). The displacements in each region are shown relative to an arbitrary point approximately in the center of each simulated region. The TFZ was affected most by the recent rifting episode since it is closest. However, substantial displacements are also predicted in the Askja area and the EVZ. The WVZ and the SISZ were also affected but to a much lesser degree than areas closer to the Krafla segment. Very little motion is predicted as far away as the Reykjanes Peninsula. Thus the effects of tectonic processes in nearby regions should be taken into account when modeling the total deformation field.

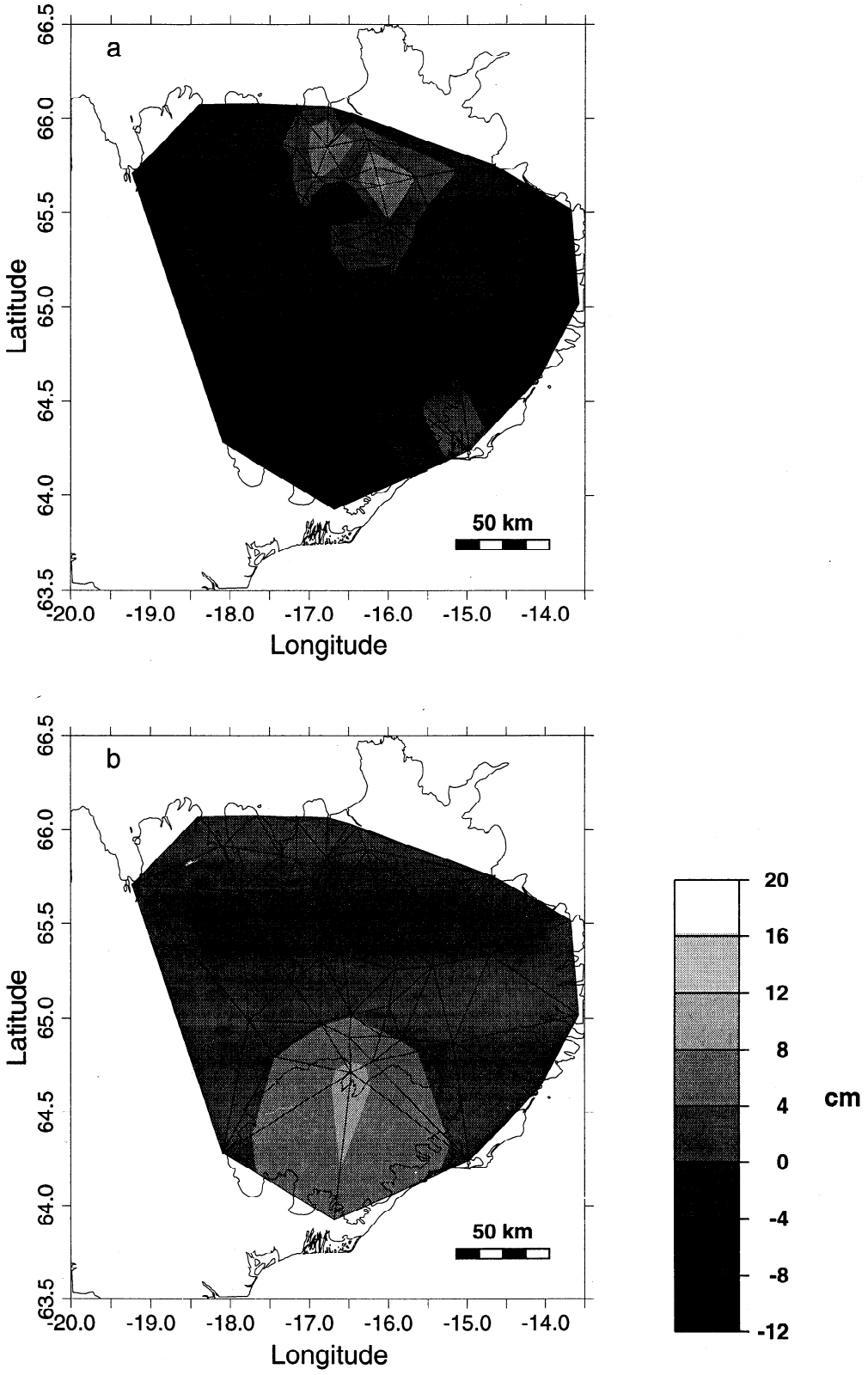

Figure 4. (a) The residual vertical deformation field for 1987–1992 after subtracting the effects of rifting events, large earthquakes, and deflations of the Askja magma chamber [*Hofton and Foulger*, this issue]. The 1σ errors are at the 2-cm level. Measurement points are located at the intersections of lines and motion in between has been estimated by bilinear interpolation. The scale bar at right gives vertical displacement in centimeters. (b) Vertical displacements for 1987–1992 predicted for points of the GPS network as a result of isostatic uplift in south Iceland following the removal of iceload during this century, estimated using the model of *Sigmundsson and Einarsson* [1992] for a viscosity of 1 x 10^{19} Pa s. The ice cap center is at 16.68°W, 64.40°N.

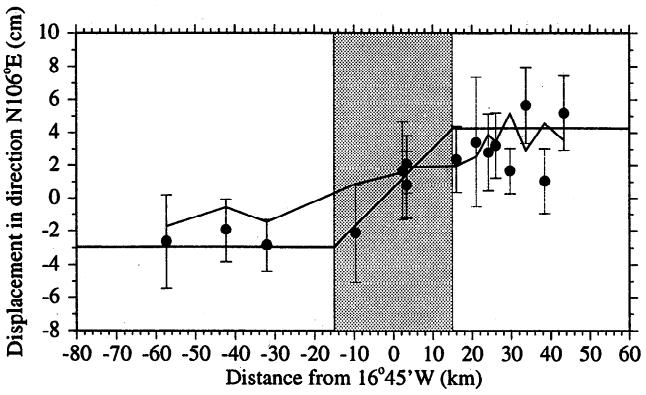

Figure 5. Observed and predicted displacements of points within the Askja region for 1987–1990 in the direction N106°E (the NUVEL-1A spreading direction) against distance. The effects of tectonic events other than the recent Krafla rifting episode have been subtracted from the observed displacements; 1σ error bars are shown. The shaded region highlights the width of the "plate boundary zone" and the solid, straight line represents the plate rate inferred by *Camitz et al.* [1995]. The irregular line indicates the displacements predicted by the model of postrifting viscoelastic relaxation following the recent Krafla rifting episode [*Hofton and Foulger*, this issue].

Implications for the Spreading Process in General

Temporal Evolution of the Large-Scale Deformation Field and Crustal Motion Rates

Large-scale, long-term deformation following dike emplacement is modeled using the elastic-viscoelastic model and an infinitely long dike. This approach is used in order to highlight some of the interesting complexities of the model only. Our representation of the plate boundary as an infinitely long dike is clearly unrealistic since plate boundaries are segmented, with intrusions rarely occurring on several segments simultaneously. In the following section the plate boundary is represented using the more realistic system of five overlapping dikes on which emplacement occurs at discrete time intervals.

The model predicts that the deformation field will vary with time. This is illustrated for the infinitely long example dike in Figures 7 and 8 over timescales of 0 to 10,000 τ_a, where τ_a is the effective relaxation time, $\tau_a = 2\eta/\mu_h$, η is the viscosity, and μ_h is the rigidity of the half-space. The elastic (codike injection) horizontal displacements are large close to the dike and decrease rapidly with distance (Figure 7a). The postdike injection response shows a general increase in accumulated

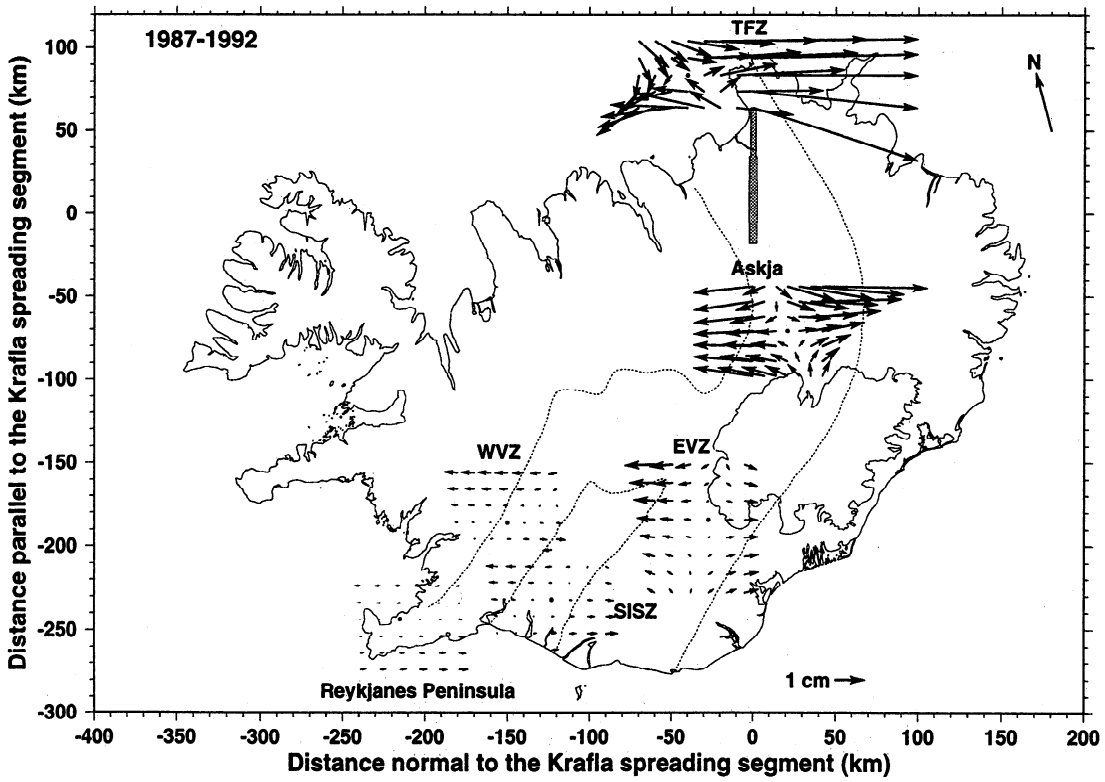

Figure 6. Predicted displacements for 1987–1992 in the Askja area, the Tjörnes Fracture Zone (TFZ), Eastern Volcanic Zone (EVZ), Western Volcanic Zone (WVZ), South Iceland Seismic Zone (SISZ), and on the Reykjanes Peninsula as a result of the recent Krafla rifting episode. The Krafla dike is shown shaded, with the Krafla volcano positioned at $x = y = 0$. The outer boundary of the neovolcanic zone is shown by the dashed line. The scale vector lower right gives the displacement in centimeters.

displacement over time at large distances. Very close to the dike (at distances less than 10 km) the initial outward direction of postdike injection displacement reverses early on, and motion is inward toward the dike thereafter. At intermediate distances (~20–150 km) the motion is complex and variable. Large displacements outward from the dike occur early on, but later ($\sim 10\tau_a$ after the event) the postdike displacement begins to decrease (Figure 7a).

Codike injection subsidence is predicted within approximately 20 km of the dike, which decreases rapidly with distance (Figure 7b). The postdike injection motion is in the opposite sense with uplift occurring in the vicinity of the dike, the amount of which increases with time. A pattern of local subsidence and uplift farther away is predicted at 10–150 km on either side of the dike that migrates out with time. No significant vertical motion is predicted farther than 150 km from the dike.

Anelastic deformation resulting from the intrusion of an infinitely long dike causes horizontal displacements outward from the dike to accumulate at all distances shortly after the intrusion (Figure 8a). This results in the rather surprising phenomenon of excess displacement in the flank areas (at distances of less than ~150 km from the dike in this case). This appears to be a result of postdike injection extension in the top of the viscoelastic region as a result of increased extensional stresses there caused by the dike emplacement. The amount of displacement in the flank areas decreases at various times, depending on distance (Figure 8a), and after a long period the accumulated displacement at all distances is approximately equal to the amount of dike opening. Within 350 km of the dike the amount of displacement is underestimated by a few percent, a result of the boundary conditions used in the model [*Hofton*, 1995].

Postdike injection anelastic vertical deformation causes the initial subsidence to decrease over time in the vicinity of the infinitely long dike (Figure 8b). Additional subsidence accumulates at distances of ~20–120 km. After a long time, net subsidence is predicted

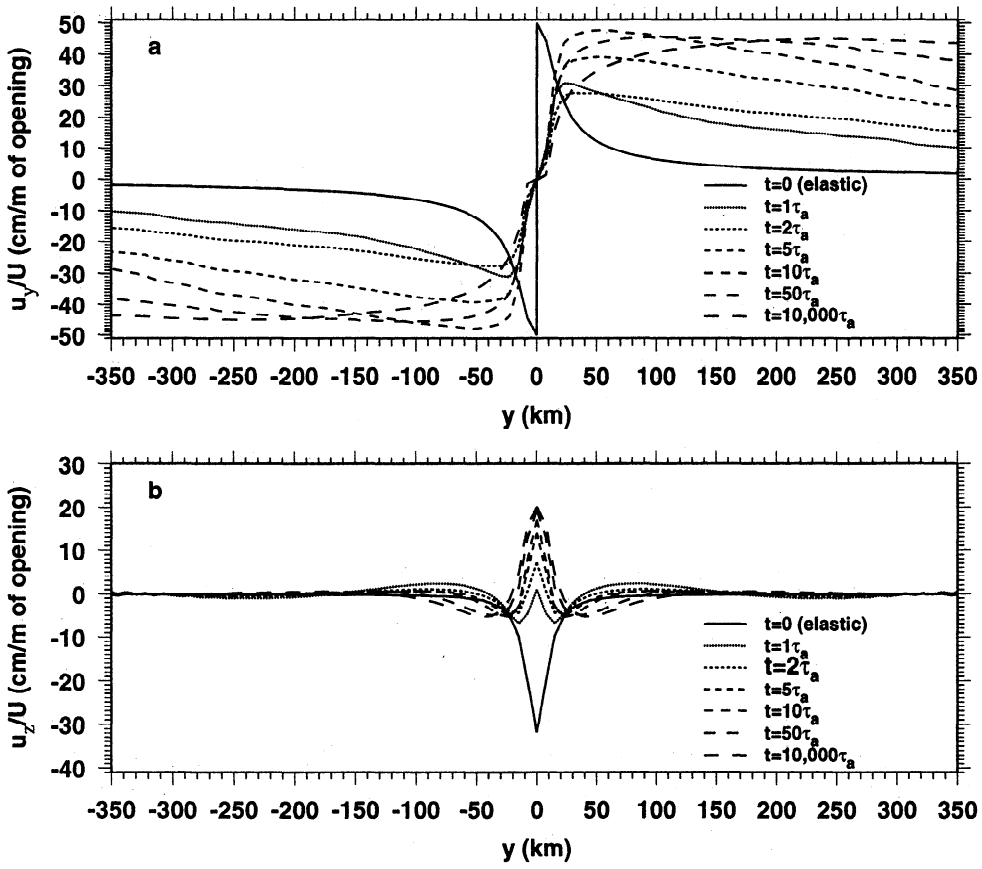

Figure 7. Predicted (a) horizontal and (b) vertical displacement including the elastic response and the postdike injection displacement ($t > 0$) due to an infinitely long dike using the elastic-viscoelastic model. Model parameters are $H = W = 10$ km, $\rho_l = 2.8$ g/cm^3, $\rho_h = 3.1$ g/cm^3, μ_l=2.7 x 10^{10} Pa, λ_l =4.9 x 10^{10} Pa, μ_h =4.1 x 10^{10} Pa, λ_h =9.9 x 10^{10} Pa, and $\psi = 90°$ [*Hofton and Foulger*, this issue]. The small oscillations in Figure 7b when $y > \pm 300$ km are due to the fineness of the integration interval, the level of which is set to produce a practical computation runtime (no more than a few hours using a Sparc station 10).

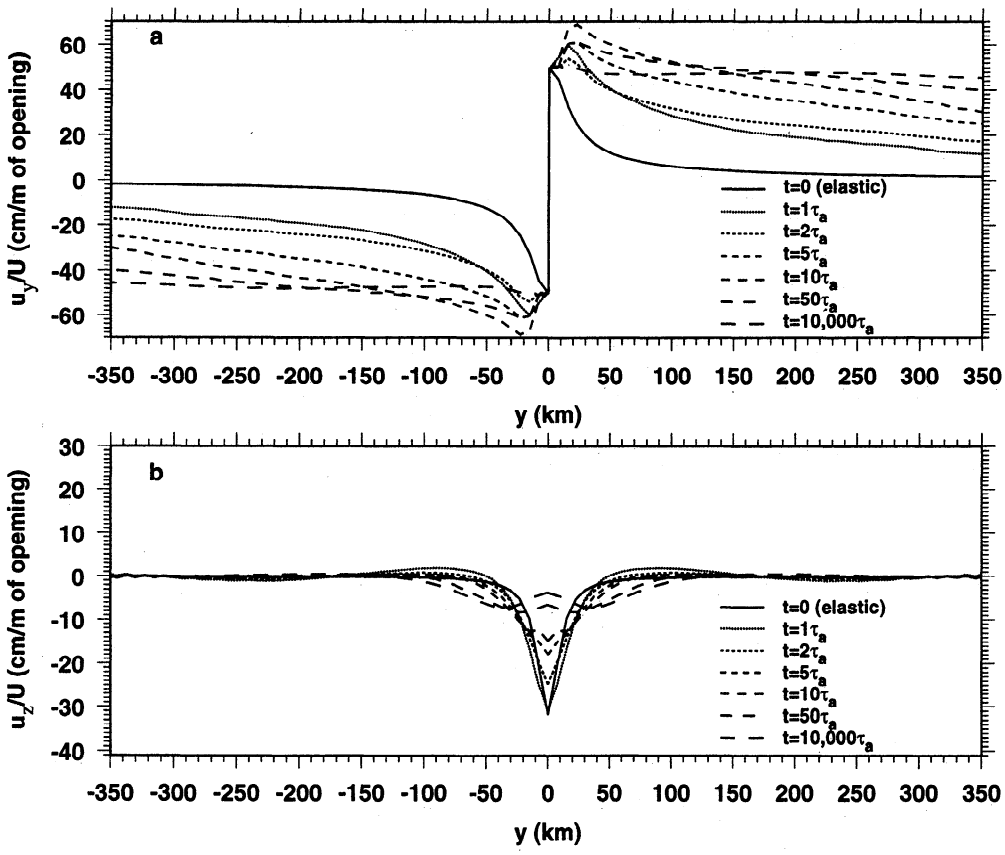

Figure 8. Same as Figure 7, except total (elastic plus viscoelastic) displacement from $t = 0$ (a) horizontal and (b) vertical.

within ~100 km of the dike, with local, relative uplift within ~20 km of the dike.

To highlight further some of the interesting complexities of the model, the evolution of the displacement field with time is illustrated (Figure 9). Following a single event on an infinitely long dike, the same amount of horizontal displacement eventually occurs everywhere as a result of stress redistribution in the viscoelastic half-space. However, the evolution of the displacement field with time depends on distance from the boundary. Close to the plate boundary very little transient motion is observed (Figure 9a), and the majority of the final displacement occurs at the time of the event. Farther away from the plate boundary (e.g., at ~15 km), the total amount of displacement increases until $\sim 10\tau_a$ after the event. The amount of displacement then decreases until $\sim 30\tau_a$ at which time the amount of displacement begins to increase again. The maximum amount of displacement occurs at $\sim 100\tau_a$ after the event and exceeds the amount of dike opening by ~35%. This general displacement pattern occurs at all points out to distances of ~150 km from the boundary, with the amplitude of the displacements decreasing with distance. Beyond distances of ~150 km from the boundary, e.g., at ~210 km, little excess displacement occurs and a simple pattern of evolution of displacement with time is predicted. There, the displacement curve can be divided into two stages. In the first stage the displacement quickly increases to near its maximum value (within $\sim 15\tau_a$ of the event). Following this the rate of motion greatly decreases as the total displacement reaches its final and maximum value over the next $\sim 50\tau_a$.

The vertical field shows that within ~120 km of an infinitely long dike, net subsidence is predicted following a single intrusion (Figures 8b and 9b). Close to the dike (within ~15 km) uplift then occurs until $\sim 25\tau_a$, at which time subsidence resumes. Uplift is again predicted after $\sim 100\tau_a$. Between 30 and 90 km from the dike axis the amount of subsidence progressively increases to a maximum at $\sim 50\tau_a$. At distances of greater than ~120 km vertical motions in response to the intrusion are small.

A deformation rate that is highly variable spatially and temporally and also varies in sign is thus predicted by the model. Close to the axis a maximum expansion rate of ~60 cm/τ_a is predicted shortly after the event (Figure 10). This quickly decreases and within $\sim 2\tau_a$ of the event, contraction at a rate of up to 10 cm/τ_a is predicted within ~120 km of the dike. The direction of motion then reverses again and at $5\tau_a$ after the event

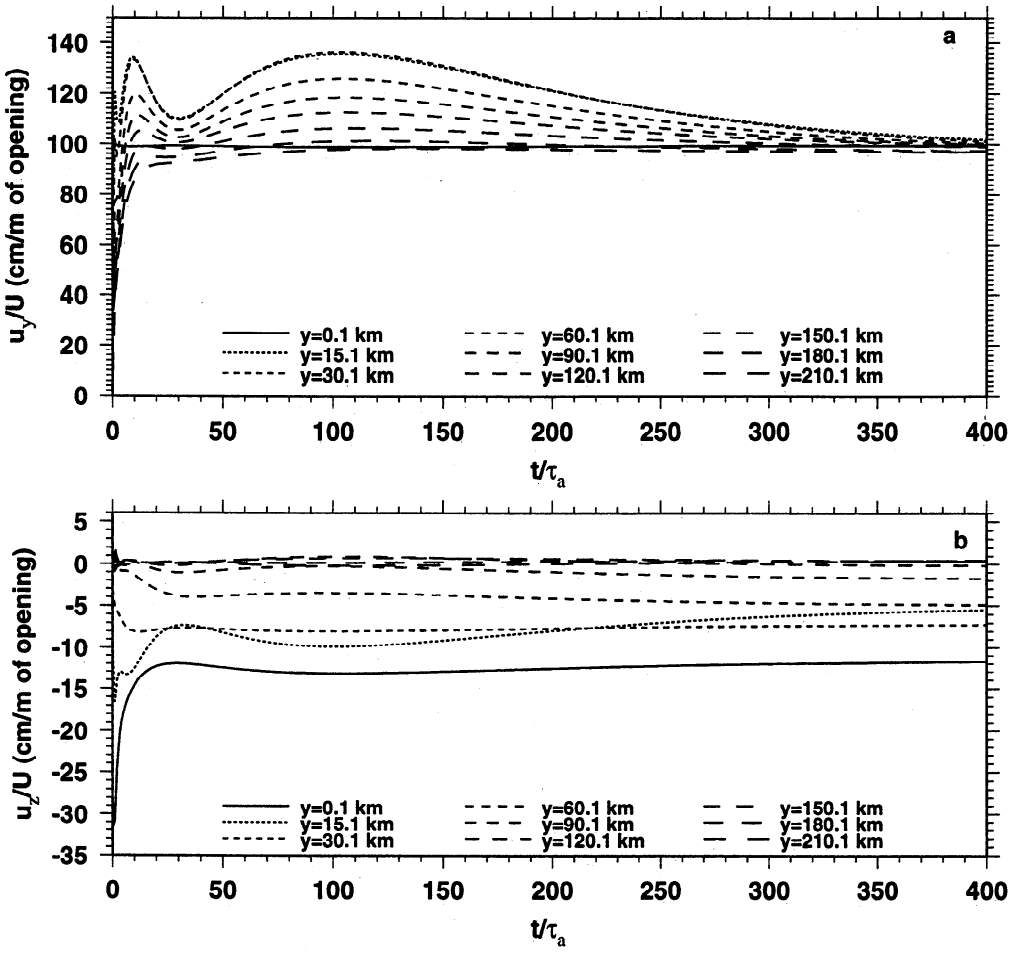

Figure 9. The variation of total displacement (elastic plus viscoelastic) with time due to a single dike injection event in (a) the horizontal and (b) the vertical direction from $t = 0$ for a suite of distances. Model parameters are identical to those used for Figure 7.

expansion at a rate of up to 9 cm/τ_a occurs. The rate of motion subsequently decreases, and at ~50 τ_a after the event it decays to ~1 cm/τ_a. The rate decreases to zero at all distances within ~100τ_a of the event. Reversals of the direction of motion occur out to distances of ~120 km.

A Segmented Plate Boundary Model

We now represent the plate boundary in north Iceland using a reasonably realistic system of five overlapping segments in which dike emplacements occur at discrete time intervals. Each dike is 120 km in length and successive dikes overlap by 20 km at each end (Figure 11a). Five meters of opening occur during each intrusion event, except in regions of overlap where 2.5 m occur. Thus, after a time 500τ_a, the total amount of opening is identical at all points along the five segments, except in the far north and south of the system, where the model terminates. In reality, the model would connect to other parts of the plate boundary, but these are not modeled here. Dike intrusions occur every 50τ_a, from t=0 to t=500τ_a (Figure 11a). The total horizontal and vertical displacements with respect to time were calculated, and profiles were plotted through the center of segment 3 (Figure 11a). This approach is a simplification of plate boundary processes and conditions. For example, only intrusions within a small (520-km-long), region of the plate boundary are modeled, other orders of dike intrusion could occur, and regional variations in structure occur in reality. However, interesting effects are illustrated by this approach.

The pattern of motion varies with time and distance from the axis (Figures 11b and 11c). Horizontal motion at the boundary is highly episodic, with most of the motion occurring at the time of an event on segment 3 and little or none when the neighboring segments spread (Figure 11b). Farther away (e.g., ~30 km from the boundary) rapid, step-like motion occurs at the time of an event on segment 3 and variable though smoother motion at the times of intrusions on other segments. At larger distances (e.g., ~90 km) from the boundary a similar though attenuated pattern of motion occurs, and at distances of over 200 km from the plate boundary, the motion when segment 3 undergoes

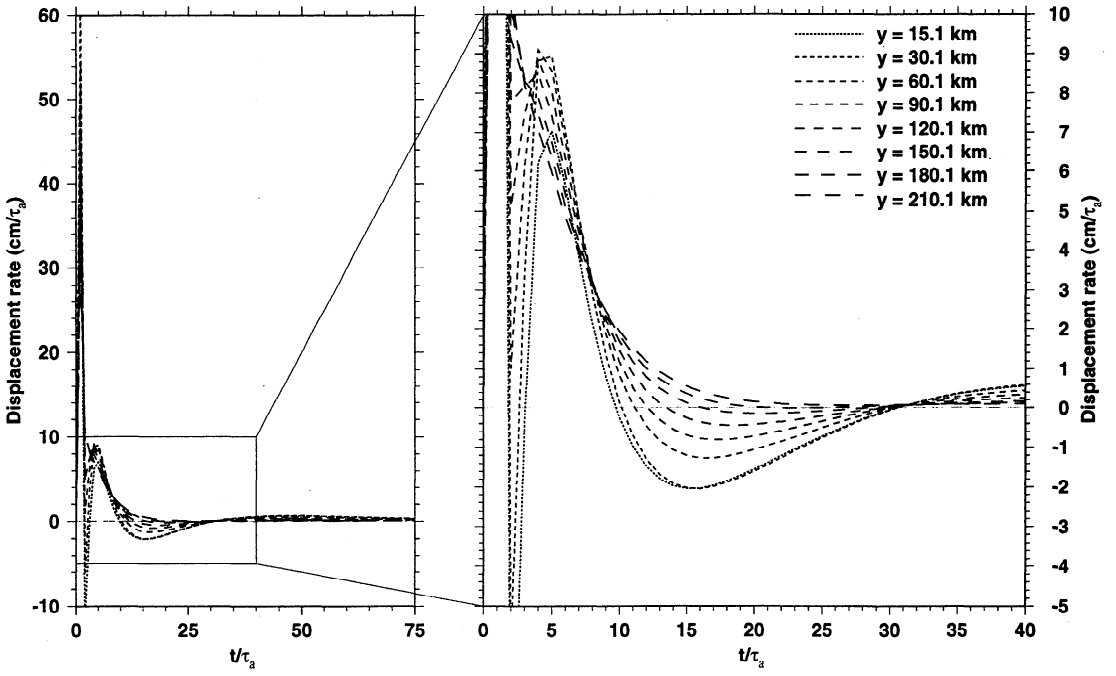

Figure 10. The variation of horizontal displacement rate with time after a single dike injection event for a suite of distances. The area enclosed by a box in the figure on the left is shown enlarged in the figure on the right. Model parameters are identical to those used for Figure 7.

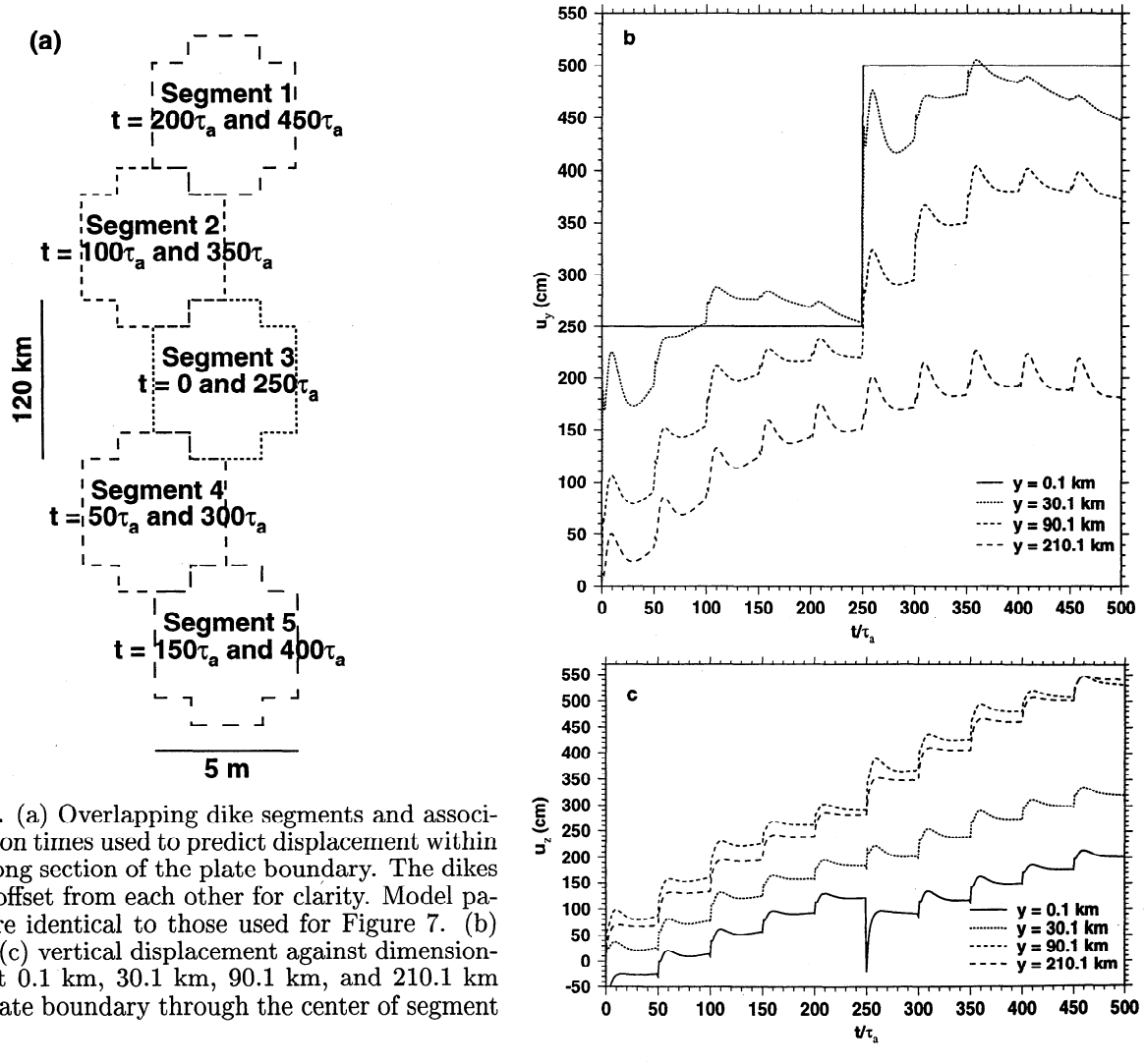

Figure 11. (a) Overlapping dike segments and associated intrusion times used to predict displacement within a 520-km-long section of the plate boundary. The dikes are shown offset from each other for clarity. Model parameters are identical to those used for Figure 7. (b) Horizontal (c) vertical displacement against dimensionless time at 0.1 km, 30.1 km, 90.1 km, and 210.1 km from the plate boundary through the center of segment 3.

intrusion is little different from that when the other segments spread.

Close to the dike subsidence is predicted at the time of an event on segment 3, with small amounts of uplift ocurring when neighboring segments spread (Figure 11c). Farther away uplift is predicted at the time of intrusions on all segments, and the pattern of motion is not greatly affected by which segment underwent spreading.

Using this model, the total horizontal displacement at all distances is not the same (Figure 11b). When $y > 0$, motion is underestimated. This is because of the absence of events outside of the modeled 520-km-long section of the plate boundary. Nevertheless, the results give valuable insights into deformation around real spreading plate boundaries. Within 200 km of the plate boundary the pattern of motion is strongly affected by which segment spread. High rates of motion occur just after spreading on the segment across which the profile is measured, and lower rates occur if a segment farther along-strike on the boundary spread. This distinction becomes small 200 km from the plate boundary. Motion is nevertheless predicted to be variable out to at least 200 km from the boundary, with rapid motion following a dike intrusion and little or none just before the next intrusion.

A relaxation time of ~1.7 years is indicated for north Iceland by the best fit model to the 1987–1992 GPS measurements [*Hofton and Foulger*, this issue]. The event recurrence time in the NVZ is thought to be about 100–150 years [*Björnsson*, 1985] and five en échelon systems exist in this region; thus our simple model is broadly analogous to the morphology and behavior of the NVZ. Recent preliminary results from GPS measurements in 1993 and 1995 indicate motion rates of up to 4 cm/year for the period 1993–1995 from -200 km to +150 km either side of the plate boundary, i.e., twice the time-averaged spreading rate (C. Völksen, personal communication, 1996). These observations support the results of this modeling.

Discussion

Crustal Deformation and Tectonics in Iceland

Postrifting viscous stress redistribution on a regional scale can explain the tilt observations in the Krafla area since 1988/1989. These tilt measurements were previously interpreted as continued activity in the Krafla magma chamber or in some deeper chamber [*Tryggvason*, 1994]. The current analysis indicates, however, that the recent phase of activity may have ended in 1988/1989. A few centimeters of uplift near to Krafla may thus have occurred as a result of magma chamber inflation there between 1987 and 1988/1989 and should be taken into account in future modeling of the 1987–1992 deformation field.

Stress redistribution following large volcano-tectonic events may be taken to indicate that the volcanic hazard is greater than it really is. This is because transient viscoelastic motion may cause surface deformations that resemble and are mistakenly interpreted as magma chamber inflation and deflation. Clearly, the contribution to surface deformation of viscous stress redistribution following the movement of molten rock subsurface, for example, into a magma chamber or forming dikes, should be taken into account before concluding that a volcano still constitutes a great volcanic hazard long after the eruptive/intrusive activity is over.

Significant, unexplained vertical motion observed around the ice cap Vatnajökull during 1987–1992 fits very poorly the model of isostatic uplift centered on the present ice cap suggested by *Sigmundsson and Einarsson* [1992]. Future measurements of the GPS points in this area to improve the accuracy of the vertical velocity field will be important in confirming or otherwise the occurrence of isostatic adjustments around Vatnajökull.

The two interpretations presented of the motion around Askja, the "continuous plate motion" model of *Camitz et al.* [1995] and that of viscous relaxation presented here, correspond respectively to kinematic and physical modeling approaches. The kinematic approach is merely a method of describing many velocity observations in greatly summarized form. It has been shown by geological studies to be appropriate for motion over very long (geologic) times, and by Very Long Baseline Interferometry (VLBI) and Satellite Laser Ranging (SLR) measurements to well describe the relative motion between distant plate interiors. The present work suggests that such an approach may be inappropriate to closely spaced points in zones bounding the plate boundary, in as much as it may fit the deformation field poorly and only at certain times, and has no predictive capability. Furthermore, such an approach gives no physical insight. The results from the Askja system for 1987–1990 demonstrate that motion that coincidentally agree approximately with the average plate rates may be observed at certain places and times between rifting episodes. The regional deformations detected in north Iceland for 1987–1992 shows that motion may deviate radically from these rates [*Foulger et al.*, 1992; *Heki et al.*, 1993; *Jahn et al.*, 1994; *Hofton and Foulger*, this issue].

The model predictions show that the effects of the recent Krafla rifting episode are significant in many parts of Iceland and should be taken into account when modeling deformation there. Other large, historical events will also contribute to current deformation in various parts of Iceland, for example, large, historical earthquakes in the SISZ.

The results of this analysis suggest that plate motion is variable out to distances of at least 200 km from the spreading plate boundary in north Iceland. Thus GPS surveying there and in similar regimes should not be directed at refining estimates of time-averaged spreading, nor should the results be interpreted as such. The time since the last very large event may be more important.

The amount by which viscoelastic stress redistribution perturbs the "continuous plate rate" becomes smaller as the relaxation time increases. Thus this process is most important for areas with low viscosity (short relaxation times) and of lesser importance where the viscosity is high (long relaxation times), e.g., continental areas.

Style of Deformation at Spreading Plate Boundaries

The pattern of deformation at spreading plate boundaries is predicted to be much more complicated than hitherto expected, including "dynamic overshoots" where the amount of displacement exceeds the amount of initial dislocation and a subsequent decrease in displacement. This pattern of motion needs to be tested by observations. If correct, it suggests that subsidiary "opposite" tectonics may occur (transient compressional deformation at spreading plate boundaries, transient extensional deformation at compressional plate boundaries). The width of the zone of cyclic stress around spreading plate boundaries may be of the order of hundreds of kilometers wide, depending on viscosity and the thickness of the elastic layer, and this has implications for tectonic interpretations of seafloor morphology and assumptions about the width of the tectonically active zone.

The periodic decreases in magnitude of horizontal motion predicted to follow dike injection is a very surprising result that is predicted by the physics of the model [*Hofton*, 1995]. The correct working of the program was verified by exhaustive tests of behavior at the limits and comparison with the analytical formulae of *Okada* [1985] [*Hofton and Foulger*, this issue]. We are therefore confident that the results are correct and not an artifact of the programming, but they are surprising and counter intuitive. Confirmation of the results by duplication using an independent method or by continued field observations of the Krafla postdike injection deformation field are thus important areas for future research.

Conclusions

1. Modeling postrifting deformation in north Iceland has important implications for local and regional processes and for the behavior of deformation around spreading plate boundaries in general.

2. The recent phase of activity of the Krafla volcano stopped in 1988/1989.

3. A slightly lower viscosity is predicted locally beneath the Krafla volcano than for north and east Iceland as a whole.

4. The 1987–1992 GPS results reported by *Hofton and Foulger* [this issue] do not support isostatic uplift centered on the ice cap Vatnajökull.

5. The elastic-viscoelastic model predicts that excess horizontal motion occurs in some areas following the emplacement of an infinitely long dike, followed by a decrease in magnitude of the motion, such that after a long time the average horizontal motion at all points is the same. Subsidence is predicted within ~120 km of the dike for a 10-km-thick elastic layer.

6. Motion out to at least 200 km from the plate boundary in north Iceland is variable, with rapid motion following a dike intrusion and the rate of motion being small just before the next intrusion. Within 200 km the pattern of motion is affected by which segment of the plate boundary spread.

Acknowledgments. Funding for this project was provided by NERC grants GR9/834 and GR9/161. M.A.H. was supported by a NERC Ph.D. studentship. We thank N. J. Kusznir for several helpful discussions. We thank A. Gudmundsson, R. Bilham, and an Associate Editor for their comprehensive reviews that greatly improved the quality of this manuscript.

References

Björnsson, A., Dynamics of crustal rifting in NE Iceland, *J. Geophys. Res., 90*, 10,151–10,162, 1985.

Björnsson, A., K. Sæmundsson, P. Einarsson, E. Tryggvason, and K. Grönvold, Current rifting episode in north Iceland, *Nature, 266*, 318–323, 1977.

Camitz, J., F. Sigmundsson, G. Foulger, C.-H. Jahn, C. Völksen, and P. Einarsson, Plate boundary deformation and continuing deflation of the Askja volcano, north Iceland, determined with GPS, 1987–1993, *Bull. Volcanol., 57*, 136–145, 1995.

DeMets, C., R. G. Gorgon, D. F. Argus, and S. Stein, Effect of recent revisions to the magnetic reversal time scale on estimates of current plate motions, *Geophys. Res. Lett., 21*, 2191–2194, 1994.

Einarsson, P., F. Sigmundsson, M. A. Hofton, G. R. Foulger and W. Jacoby, An experiment in glacio-isostacy near Vatnajökull, Iceland, 1991, *Jökull*, in press, 1996.

Foulger, G. R., C.-H. Jahn, G. Seeber, P. Einarsson, B. R. Julian and K. Heki, Post-rifting stress relaxation at the divergent plate boundary in Northeast Iceland, *Nature, 358*, 488–490, 1992.

Grove, J. M., *The Little Ice Age*, Routledge, New York, 1988.

Gudmundsson, A., The geometry and growth of dykes, in *Physics and Chemistry of Dykes*, edited by G. Baer and A. Heimann, pp. 23–44, A. A. Balkema, Rotterdam, Netherlands, 1995.

Heki, K., G. R. Foulger, B. R. Julian, and C. -H. Jahn, Plate dynamics near divergent plate boundaries: Geophysical implications of post-rifting crustal deformation in NE Iceland, *J. Geophys. Res., 98*, 14,279–14,297, 1993.

Hofton, M. A., Anelastic surface deformation in Iceland detected using GPS, with special reference to isostatic rebound and the 1975-1985 Krafla rifting episode, Ph.D. thesis, 259 pp., Univ. of Durham, Durham, England, 1995.

Hofton, M. A., and G. R. Foulger, Postrifting anelastic deformation around the spreading plate boundary, north Iceland, 1, Modeling of the 1987–1992 deformation field using a viscoelastic Earth structure, *J. Geophys. Res.*, this issue.

Jahn, C.-H., G. Seeber, G. R. Foulger, and P. Einarsson, GPS epoch measurements spanning the mid-Atlantic plate boundary in northern Iceland 1987–1990, in *Gravimetry and Space Techniques Applied to Geodynamics and Ocean Dynamics, Geophys. Monogr. Ser.*, vol. 82, edited

by B. E. Schutz et al., pp. 109–123, AGU, Washington, D. C., 1994.

Okada, Y., Surface deformation due to shear and tensile faults in a half-space, *Bull. Seismol. Soc. Am., 75*, 1135–1154, 1985.

Sigmundsson, F., and P. Einarsson, Glacio-isostatic crustal movements caused by historical volume change of the Vatnajökull ice cap, Iceland, *Geophys. Res. Lett., 19*, 2123–2126, 1992.

Sigurdsson, H., and R. S. J. Sparks, Rifting episode in north Iceland in 1874–1875, and the eruption of Askja and Sveinagjá, *Bull. Volcanol., 41*, 149–167, 1978.

Tryggvason, E., Widening of the Krafla fissure swarm during the 1975–1985 volcano-tectonic episode, *Bull. Volcanol., 47*, 47–69, 1984.

Tryggvason, E., Surface deformation at the Krafla volcano, north Iceland, 1982–1992, *Bull. Volcanol., 56*, 98–107, 1994.

G. R. Foulger, Department of Geological Sciences, University of Durham, South Road, Durham, DH1 3LE, England.

M. A. Hofton, IGPP/UCSD, Dept. 0225, 9500 Gilman Drive, La Jolla, CA 92093. (e-mail: mhofton@ucsd.edu)

(Received November 1, 1995; revised May 1, 1996; accepted July 29, 1996.)